

RNA-dependent Folding and Stabilization of C5 Protein During Assembly of the *E. coli* RNase P Holoenzyme

Xia Guo³, Frank E. Campbell^{1,2}, Lei Sun^{1,2}, Eric L. Christian^{1,2},
Vernon E. Anderson² and Michael E. Harris^{1,2*}

¹Center for RNA Molecular Biology, Case Western Reserve University School of Medicine Cleveland, OH 44118, USA

²Department of Biochemistry Case Western Reserve University School of Medicine Cleveland, OH 44118, USA

³School of Chemistry and Chemical Engineering Yangzhou University, Yangzhou Jiangsu 225002, P.R. China

The pre-tRNA processing enzyme ribonuclease P is a ribonucleoprotein. In *Escherichia coli* assembly of the holoenzyme involves binding of the small (119 amino acid residue) C5 protein to the much larger (377 nucleotide) P RNA subunit. The RNA subunit makes the majority of contacts to the pre-tRNA substrate and contains the active site; however, binding of C5 stabilizes P RNA folding and contributes to high affinity substrate binding. Here, we show that RNase P ribonucleoprotein assembly also influences the folding of C5 protein. Thermal melting studies demonstrate that the free protein population is a mixture of folded and unfolded conformations under conditions where it assembles quantitatively with the RNA subunit. Changes in the intrinsic fluorescence of a unique tryptophan residue located in the folded core of C5 provide further evidence for an RNA-dependent conformational change during RNase P assembly. Comparisons of the CD spectra of the free RNA and protein subunits with that of the holoenzyme provide evidence for changes in P RNA structure in the presence of C5 as indicated by previous studies. Importantly, monitoring the temperature dependence of the CD signal in regions of the holoenzyme spectra that are dominated by protein or RNA structure permitted analysis of the thermal melting of the individual subunits within the ribonucleoprotein. These analyses reveal a significantly higher T_m for C5 when bound to P RNA and show that unfolding of the protein and RNA are coupled. These data provide evidence for a general mechanism in which the favorable free energy for formation of the RNA–protein complex offsets the unfavorable free energy of structural rearrangements in the RNA and protein subunits.

© 2006 Elsevier Ltd. All rights reserved.

*Corresponding author

Keywords: ribonucleoprotein; RNase P; C5 protein; circular dichroism

Introduction

Ribonucleoprotein assembly is nearly always accompanied by changes in the conformation of the interacting RNA or protein, or both.^{1–3} An extreme example is assembly of the ribosome, which involves the sequential binding of numerous proteins *via* multiple pathways leading to large-scale changes in the conformation of the associated RNA and proteins.^{4–7} Structural studies of a growing number of RNA-binding proteins and their cognate RNAs reveal numerous modes of binding and a wide range of conformational changes associated with assembly.³ Comparison of the structures of the

free and bound states of RNA and protein provides essential insights on the degree of molecular rearrangement that occurs and also suggests likely trajectories for large-scale molecular motion. Yet, additional information is clearly necessary to define the relationships between conformational changes and essential aspects of biological function such as affinity or specificity. Thus, defining the kinds of structural changes that occur during the assembly of functionally important cellular ribonucleoproteins and understanding how they are linked to function remain important goals.

The tRNA processing endonuclease RNase P is an essential and ubiquitous ribonucleoprotein in which functional collaboration between its RNA and protein subunits is essential for its physiological function,^{8–10} yet relatively little is known about how the active holoenzyme is assembled. In Bacteria, the

E-mail address of the corresponding author:
michael.e.harris@case.edu

composition of the complex is simple, consisting in *Escherichia coli* of one 377 nucleotide RNA (P RNA) and a single 119 amino acid residue protein subunit (C5). The large P RNA encompasses the majority of the binding interface for the pre-tRNA substrate including the active site. P RNA alone can fold in the presence of magnesium ions into a conformation that can catalyze pre-tRNA cleavage, but binds the substrate with low affinity. The C5 protein binds within the catalytic domain of P RNA,^{11–13} and this association results in important changes in the functional properties of the enzyme^{9,14} (Figure 1(a)). Biochemical and structure probing analyses show that the protein contributes to pre-tRNA binding by interacting directly with 5' leader sequences adjacent to the cleavage site. Additionally, the protein subunit enhances the binding affinity of metal ions important for substrate cleavage.^{15–17}

Evidence for changes in P RNA structure that may be related to protein effects on function come from chemical probing experiments that show a greater degree of protection by the protein subunit than can be accounted for by its relatively small size.^{20,21} Furthermore, enhancements to chemical modification and interference observed in the presence of the protein are also consistent with changes in RNA structure.¹³ Recent physical studies of the RNA subunit by Pace and colleagues demonstrate that protein binding alters the structure of P RNA, which appears to result in additional, or stronger RNA–RNA interactions with tRNA.¹⁸ Consistent with this model is the ability of C5 to suppress the effects of some mutations in P RNA that disrupt tertiary structure.¹⁹ Unfortunately, the interface between the RNA and protein subunits remains poorly defined. Additionally, although models can be built in which the protein interacts with the catalytic domain, as well as the leader sequence of a docked substrate,²¹ a high-resolution structure of the complex is lacking. Thus, while functional and structural changes in the RNA subunit brought about by protein binding may explain in part why C5 is essential *in vivo*, the kinds of changes in conformation that are induced by the protein, as well as the manner in which RNA conformations and function are linked at the molecular level remain poorly understood.

Achieving a complete description of RNase P assembly will necessarily involve understanding not only conformational changes in P RNA, but also the extent of conformational changes in the protein subunit. The structures of the free protein have been determined for three different bacteria revealing a conserved alpha/beta sandwich fold^{22–24} (Figure 1(b)). Comparative sequence analysis identifies conserved basic residues, as well as hydrophobic residues in a cleft formed by $\alpha 2$ and $\beta 1-3$ that are important for RNA binding and function.^{23,25} However, as indicated above, the interface between the RNA and protein subunits is not yet well defined, and it is not known whether the structure of the protein changes when the P RNA is bound. Evidence that RNA binding may influence RNase P protein folding is provided by recent physical

studies of the *Bacillus subtilis* RNase P protein by Oas and colleagues demonstrating that protein folding is linked to anion binding.²⁶ These physical analyses provide evidence for a mechanism involving binding of anions to the folded state of the protein. Folding was induced best by polyvalent phosphate ions, suggesting a role for the RNA phosphodiester backbone in protein stabilization. These observations raise important questions with regard to RNase P assembly, in particular how RNA binding influences the conformation and folding of the protein subunit and how, or whether, changes in conformation of the RNA and protein subunits are linked.

Results

Stoichiometric assembly of *E. coli* RNase P holoenzyme

To better understand the assembly of the *E. coli* RNase P ribonucleoprotein we undertook a series of equilibrium spectroscopic analyses to identify differences in the conformation of the free and bound protein subunit. Historically, an impediment to physical and biochemical analyses of the *E. coli* RNase P holoenzyme has been the low specific activity of purified C5 protein, and it has been commonly added in excess to insure efficient holoenzyme assembly.^{25,27,28} For this study we purified highly active C5 in quantities that are sufficient for physical analyses of holoenzyme assembly using a well-characterized system of affinity purification that relies upon expression of C5 as a fusion protein with a chitin-binding domain. Removal of the affinity tag by intein cleavage yields a protein with the precise C5 amino acid sequence (see Materials and Methods). SDS-PAGE of protein samples from over-expressing cells and fractions from the purification are shown in Figure 2(a). Induction of expression results in the accumulation of a protein at the molecular mass expected for the fusion protein (71.3 kDa). Affinity purification and intein cleavage result in elution of highly purified protein that migrates at the appropriate molecular mass (13.8 kDa). Mass spectrometric analyses confirm the identity of the protein as full-length C5 protein (data not shown). The protein alone shows no activity in pre-tRNA processing *in vitro*, and inspection of the UV and CD spectra reveals no detectable contamination by nucleic acid, indicating that the protein preparation is free of contaminating P RNA (data not shown).

To determine the fraction of the purified protein capable of forming functional complexes with P RNA we titrated C5 into pre-tRNA processing reactions containing a constant concentration (25 nM) of the RNA subunit. RNase P assembly and enzyme activity are highly sensitive to ionic strength; these and subsequent experiments were conducted under standard monovalent and divalent

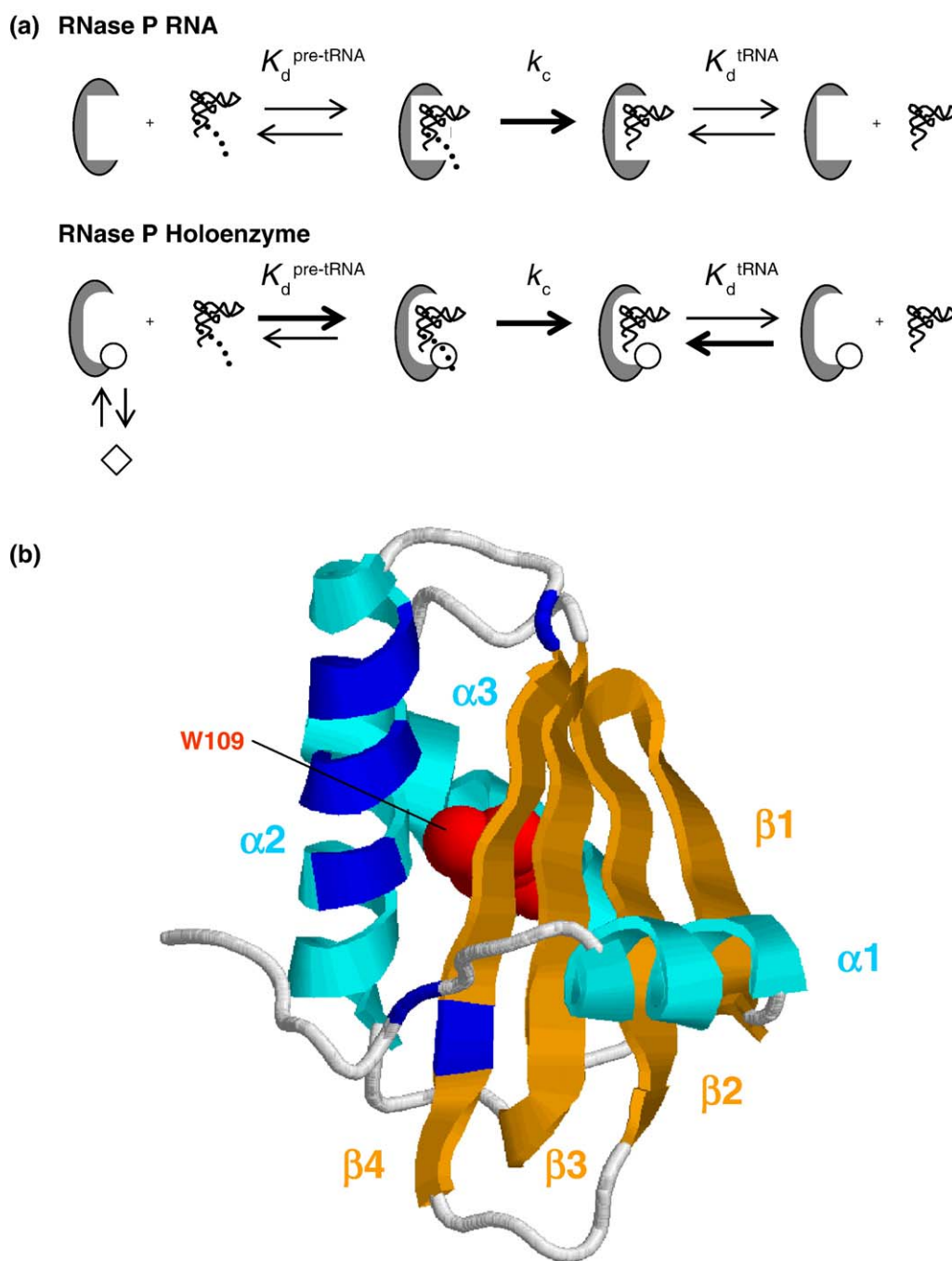


Figure 1. Functional contributions and three-dimensional structure of bacterial RNase P protein. (a) Functional contributions of the RNA and protein subunits of bacterial RNase P. The free RNA subunit is shown as a grey oval while the free protein subunit is depicted as a white diamond. P RNA and C5 protein bound to form the RNase P holoenzyme are shown as an oval with smooth contours for the substrate-binding site and a circle, respectively, to indicate the conformational changes that occur upon assembly. The tRNA portion of the substrate is shown in backbone representation and the 5' leader sequence is represented by a dotted line. Protein binding leads to improvement in substrate binding ($K_d^{\text{pre-tRNA}}$) in part due to interactions with the 5' leader, but there is little effect on the substrate cleavage step (k_c). Additionally, the protein enhances interactions with the tRNA (K_d^{tRNA}) that are linked to conformational changes in the RNA subunit.²⁷ (b) Structure of RNase P protein from *B. subtilis*²³ (PDB 1A6f). The identities of conserved secondary structure elements are indicated. The locations of conserved basic residues that are believed to play a role in interactions with the RNase P RNA subunit are shown in dark blue. The homologous position of W109 in the *B. subtilis* structure is shown in red.

ion concentrations of 100 mM NaCl and 17 mM MgCl₂ unless indicated otherwise. Under these conditions there is essentially no detectable pre-

tRNA^{ASP} processing activity observed with P RNA alone, which is attributable to very low substrate binding affinity. Increasing the concentration of C5

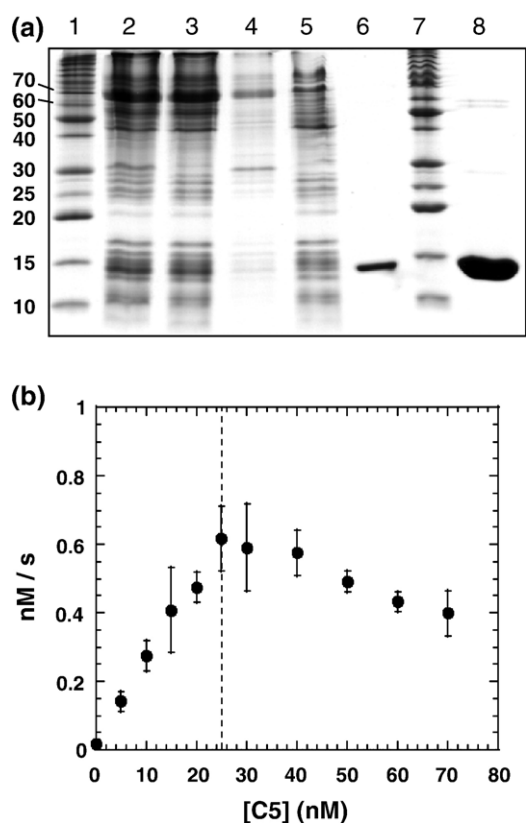


Figure 2. Purification of *E. coli* RNase P protein (C5) and stoichiometric assembly of the holoenzyme. (a) SDS-PAGE analysis of protein samples from over-expressing cells and affinity column fractions. RNase P protein was over-expressed as a fusion with chitin-binding domain as described in Materials and Methods. Lanes 1 and 7, Benchmark Protein ladder molecular weight standards (Invitrogen) with sizes in kiloDaltons indicated to the left; lanes 2, 3 and 4, whole cell lysate from an induced culture, the soluble fraction of this lysate, and the insoluble fraction of this lysate, respectively; lane 5, flow-through of chitin column during loading of the clarified lysate; lanes 6 and lane 8, 1 μ g and 10 μ g, respectively of the final purified C5 preparation. The amount of sample loaded in each of lanes 2–5 represents equivalent numbers of cells. (b) Stoichiometry of RNase P holoenzyme assembly. Purified C5 protein was titrated into reactions containing 250 nM radiolabeled substrate and 25 nM P RNA (indicated by a broken line in the graph) under standard reaction conditions (see Materials and Methods). The graph shows the average observed multiple turnover rate constant (k_{obs}) from at least three independent measurements as a function of C5 protein concentration. Error bars represent one standard deviation.

results in a corresponding increase in the multiple turnover rate. The rate reaches a maximum at ca 25–30 nM C5 providing a conservative estimate that >80% of the protein can bind productively to the RNA subunit (Figure 2(b)). Increasing the C5 concentration beyond 30 nM results in a detectable decrease in rate. Equilibrium binding studies using radiolabeled RNA show that the protein subunit alone will bind weakly ($K_{\text{d,app}}$ ca 200 nM) to pre-

tRNA (data not shown) suggesting that inhibition by excess protein is due to non-specific binding to the substrate or enzyme RNAs.

Next, we characterized the effect of protein binding on molecular recognition and catalysis by comparing the substrate and product binding affinities, as well as the single turnover rate constant for pre-tRNA cleavage of both the holoenzyme and the P RNA alone. As shown in Figure 3(a), thermodynamic analyses demonstrate that binding of C5 increases pre-tRNA affinity as expected based on previous studies.⁹ Under the conditions of 100 mM NaCl and 17 mM MgCl₂ used here, the RNA alone has an apparent dissociation constant

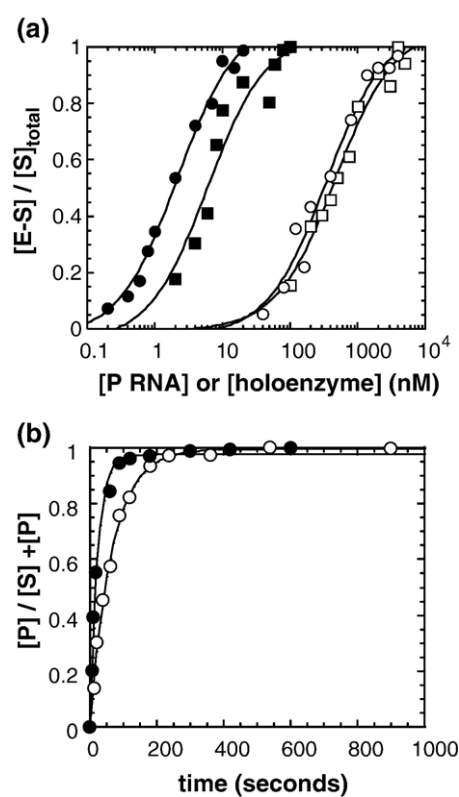


Figure 3. Effect of C5 on substrate-binding affinity, product-binding affinity and catalytic rate. (a) Equilibrium binding analysis of the affinity of P RNA and the RNase P holoenzyme for pre-tRNA^{ASP} and tRNA^{ASP}. Fractions of bound substrate were determined by gel-filtration chromatography under conditions of 50 mM Mes (pH 5.75), 100 mM NaCl and 17.5 mM CaCl₂ as described in Materials and Methods. Representative binding data for the interaction of pre-tRNA (circles) and tRNA (squares) with the RNase P RNA subunit alone (open symbols) or the reconstituted holoenzyme (filled symbols) are shown. (b) Determination of the single turnover rate constants for cleavage of pre-tRNA^{ASP} by the *E. coli* RNase P holoenzyme and P RNA alone. Single turnover reactions in 50 mM Mes (pH 5.75), 100 mM NaCl, 17.5 mM MgCl₂ with saturating concentrations of enzyme were performed, and the fraction of reacted substrate is plotted as a function of time. Representative data for the RNase P RNA subunit alone (open symbols) or the reconstituted holoenzyme (filled symbols) are shown.

($K_{d,app}$) for the model substrate, pre-tRNA^{ASP}, of >500 nM, while the protein increases this affinity by ca 500-fold ($K_{d,app} = 1.5(\pm 0.4)$ nM). Additionally, we observe a marked effect of the protein subunit on tRNA binding affinity (70-fold) with an apparent $K_{d,app}$ of 560(± 70) nM and 7.3(± 1.5) nM for binding of tRNA^{ASP} by the ribozyme and holoenzyme, respectively, which is consistent with recent quantitative studies of the contribution of the C5 protein.¹⁸ In contrast to binding affinity, kinetic analyses reveal relatively little contribution of C5 to catalysis for this substrate (Figure 3(b)). Under these standard reaction conditions the single turnover cleavage rate of the *E. coli* holoenzyme is sensitive to pH, consistent with the cleavage step being rate-limiting (data not shown). At saturating concentrations of either RNA subunit alone or the holoenzyme the observed single turnover rate is within threefold ($0.68(\pm 0.08)$ min⁻¹ versus $2.00(\pm 0.3)$ min⁻¹, for the ribozyme and holoenzyme, respectively).

Thus, the population of purified C5 assembles stoichiometrically with P RNA resulting in significant increases in pre-tRNA and tRNA binding affinity attributable to stabilization of the structure of the RNA subunit.¹⁸ Together these results demonstrate robust and quantitative incorporation of purified RNA and protein subunits into functional RNase P holoenzyme over a wide range of RNA and protein concentrations. Importantly, this system provides a well-defined arena for physical studies of RNase P holoenzyme assembly.

Spectroscopic evidence for conformational changes in C5 protein during holoenzyme assembly

To test for changes in protein structure associated with ribonucleoprotein assembly, we first examined the extent of secondary structure in the free protein population by analyzing the circular dichroism (CD) spectrum of C5. The CD spectra of C5 in buffer alone and under standard holoenzyme assembly conditions of 100 mM NaCl and 17 mM MgCl₂ at 20 °C are shown in Figure 4(a). Importantly, the spectra are significantly different with a much larger CD signal in the presence of NaCl and MgCl₂ consistent with anion-induced folding as observed for the *B. subtilis* protein.²⁶ Titration experiments demonstrate that a concentration of 100 mM NaCl alone was sufficient to result in the complete change in the CD signal, indicating that the reaction conditions used for holoenzyme assembly include concentrations of anions that are saturating for folding (data not shown). A simple model would be that holoenzyme assembly involves interaction of the RNA with a population of C5 that is already folded by anion binding. However, thermal melting studies suggest that this mechanism may not necessarily apply under all conditions. Characterization of the thermal stability of the C5 population under standard holoenzyme reaction conditions yielded the temperature dependence of the CD signal at 222 nm shown in Figure 4(b). Fitting of the data to a model

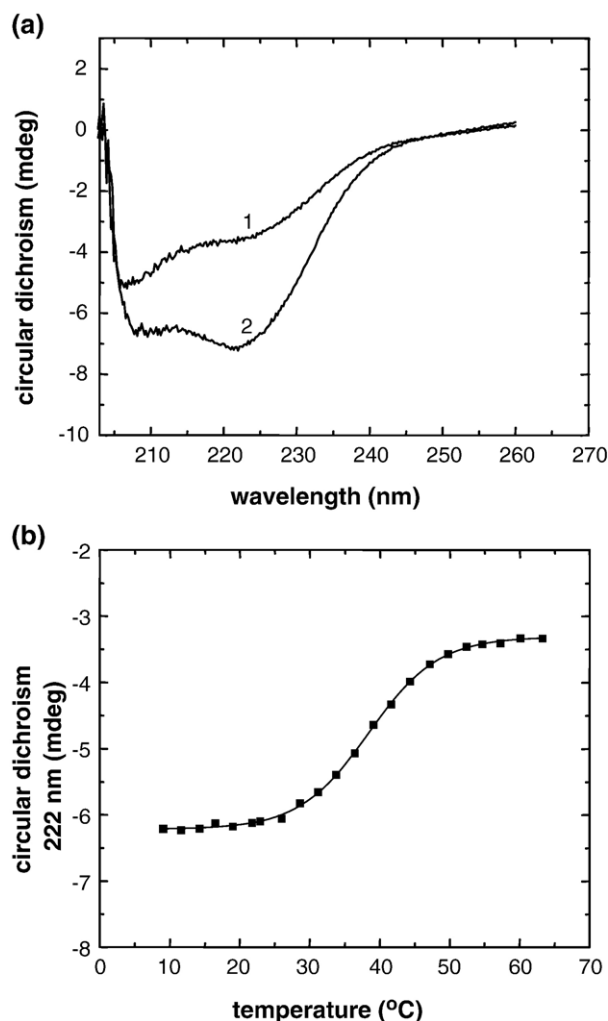


Figure 4. Characterization of C5 protein folding and thermal stability by CD spectroscopy. (a) CD spectrum of 1.5 μ M C5 protein at 20 °C in 20 mM sodium cacodylate buffer (pH 7.5) in the absence (1) and presence (2) of 100 mM NaCl and 17 mM MgCl₂. (b) Thermal denaturation spectra (from 10 °C–60 °C) monitored at 222 nm of 1.5 μ M C5 protein in 20 mM sodium cacodylate buffer (pH 7.5), 100 mM NaCl, 17 mM MgCl₂.

for a two-state folding equilibrium shows a T_m of ca 38 °C for the free C5 protein. Folding is reversible at temperatures near the T_m (data not shown). Surprisingly, the apparent T_m is remarkably lower than that for the *B. subtilis* protein under similar conditions (66 °C).²⁶ These data indicate that the population of C5 protein in the absence of P RNA exists as a mixture of both folded and unfolded states under reaction conditions in which stoichiometric holoenzyme assembly is achieved. Thus, assembly of the functional *E. coli* RNase P holoenzyme under these conditions must necessarily involve folding of a significant fraction of the protein population.

To test the idea that the presence of P RNA results in changes in the conformation of C5 we took

advantage of the intrinsic fluorescence of a single tryptophan residue (W109) located near the C terminus of the protein (Figure 1(b)). Comparison of the available structures of RNase P proteins together with an alignment of available protein sequences shows that W109 is located in an alpha helix opposite the binding face for the 5' leader sequence.^{29,30} The identity of this position is not well conserved and its role appears to be to interact with other hydrophobic amino acids in the folded core.³¹ Mutation of a conserved phenylalanine (F72) located in the hydrophobic core of C5 to alanine results in changes in the emission spectrum of W109.³¹ In contrast, mutation of the conserved F18 that is located in the binding cleft of the 5' leader sequence does not affect W109 fluorescence. Thus, W109 is not thought to form the primary binding site for the P RNA, or to be involved in pre-tRNA binding. Hence, changes in the intrinsic protein fluorescence are likely to reflect the formation of, or changes in, the structure of the folded C5 protein.

As shown in Figure 5(a), comparison of the equilibrium spectra of the free and bound protein demonstrates that W109 fluorescence is significantly increased in the presence of the RNA subunit. Excitation of free C5 protein at 280 nm yields a broad emission peak with a maximum at 327 nm. The emission spectrum as well as the excitation spectrum of C5 monitored at 327 nm (data not shown) is consistent with that of tryptophan³². Importantly, addition of a stoichiometric amount of P RNA results in a significant increase in the total fluorescence intensity. The magnitude of the change in fluorescence is quite large (ca 100%), indicating a significant change in the environment of W109 consistent with desolvation and burying of W109 in the hydrophobic core of the protein. As shown in Figure 5(b), the change in W109 fluorescence is dependent on P RNA concentration. Notably, the maximal increase in fluorescence is observed at stoichiometric concentrations of the RNA and protein, and addition of excess RNA does not result in a further increase in fluorescence intensity. These data also support the 1:1 stoichiometry of the holoenzyme suggested by the activity assay in Figure 2(b) and, importantly, are consistent with a significant change in the conformation of the protein population in the presence of P RNA.

Spectroscopic evidence for conformational changes in *E. coli* RNase P RNA during holoenzyme assembly

To better understand the structural changes in C5 protein, as well as P RNA, that accompany RNase P holoenzyme assembly, we compared the CD spectra of the free RNA and protein subunits with that of the holoenzyme. Changes in RNA and protein structure can result in changes in their CD signal; thus, evaluation of difference spectra derived from subtracting the signals of the free RNA and protein subunits from that of the complex provides information about how assembly affects their conforma-

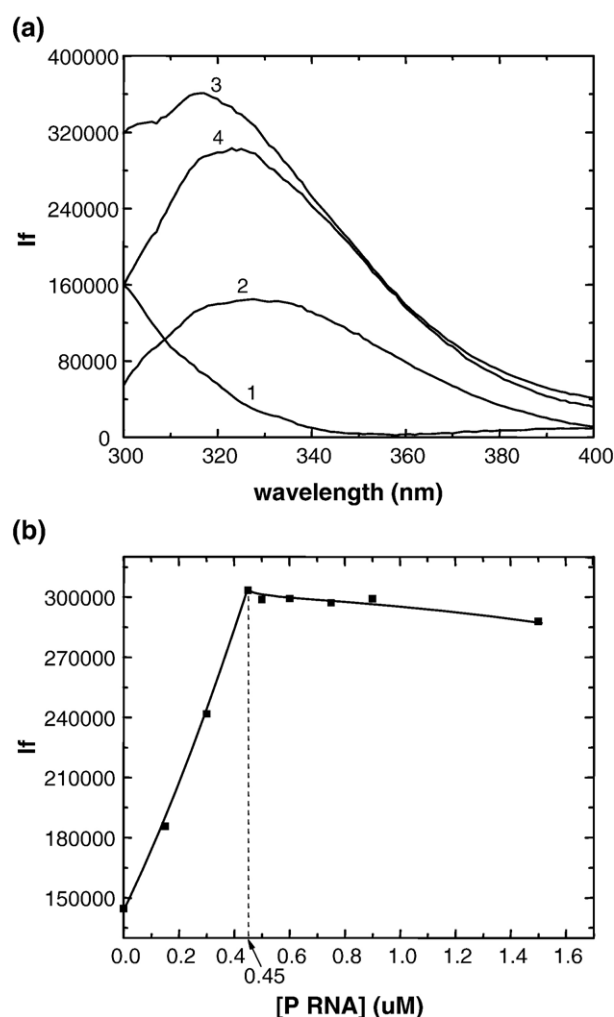


Figure 5. Effects of holoenzyme assembly on the intrinsic fluorescence of W109. (a) Fluorescence emission spectra resulting from excitation at 280 nm of 0.5 μM P RNA alone (1), 0.5 μM C5 protein alone (2), and 0.5 μM RNase P holoenzyme (3) in 20 mM sodium cacodylate buffer (pH 7.5), 100 mM NaCl, 17 mM MgCl_2 at 37 $^\circ\text{C}$. Intensities are reported as intrinsic fluorescence units (I_f). Curve 4 shows the difference spectrum resulting from subtracting the signal of the RNA alone from that of the holoenzyme. (b) Effect of P RNA concentration on the fluorescence intensity (I_f) of W109 at a fixed concentration of C5 protein (0.45 μM). The broken line indicates the concentration at which the concentrations of RNase P RNA and protein are equal.

tion. Due to the much larger size of P RNA and the greater CD signal of nucleic acids, the spectrum of the RNA subunit dominates that of the protein. As shown in Figure 6(a) for both the free RNA (curve 1) and bound RNA (curve 2), there is a strong maximum at 265 nm, a small negative signal at ~235 nm and a significant negative peak at ~210 nm. These spectra are consistent with the presence of a highly structured RNA with a significant amount of A-form helix.³³⁻³⁶ Importantly, the difference spectrum (curve 4) derived

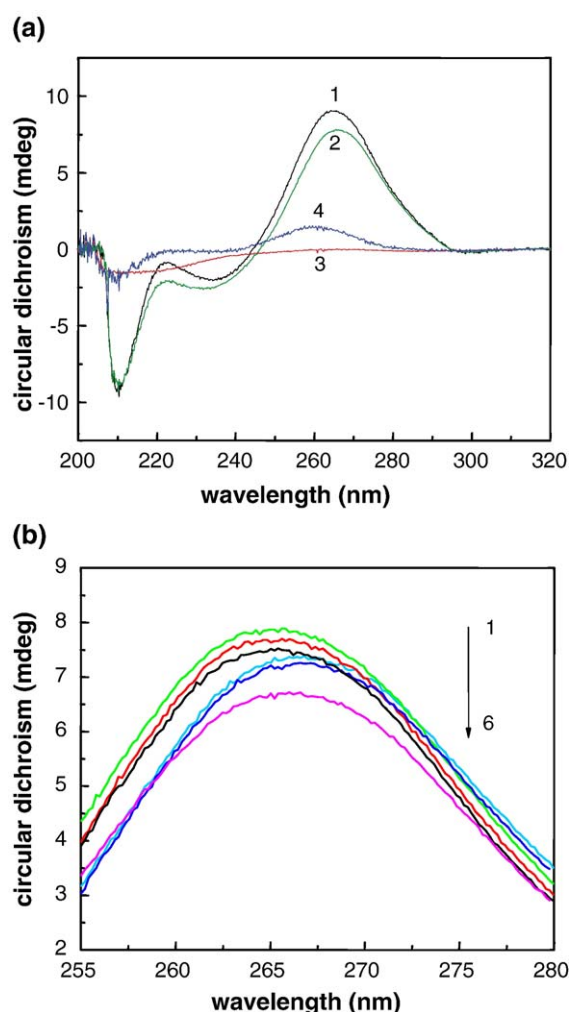


Figure 6. Effects of holoenzyme assembly on CD spectra of P RNA and protein subunits. (a) CD spectra of 0.5 μM P RNA (curve 1, black), C5 protein (curve 3, red) and the RNase P holoenzyme (curve 2, green) at 37 $^{\circ}\text{C}$ in 20 mM sodium cacodylate (pH 7.5), 100 mM NaCl, 17 mM MgCl_2 . Curve 4 (blue) is the difference spectrum obtained by subtracting the CD signal of the holoenzyme from the sum of those of the free RNA and protein subunits. (b) Effects of monovalent and divalent ions on protein-dependent changes in the CD spectrum of P RNA. All samples were obtained at 37 $^{\circ}\text{C}$ in 20 mM sodium cacodylate (pH 7.5). Curve 1 (green), 0.5 μM P RNA, 17 mM MgCl_2 ; curve 2 (red), 0.5 μM P RNA, 100 mM NaCl; curve 3 (black), 0.5 μM P RNA, 0.5 μM C5 protein, 100 mM NaCl; curve 4 (light blue), 0.5 μM P RNA alone; curve 5 (dark blue), 0.5 μM P RNA, 0.5 μM C5 protein, no MgCl_2 or NaCl; curve 6 (magenta), 0.5 μM P RNA, 0.5 μM C5 protein, 17 mM MgCl_2 .

from subtracting the signal of the ribonucleoprotein (curve 2) from the combined spectra for free RNA (curve 1) and protein (curve 3) reveals changes in the CD signal at 260 nm attributable to complex formation. Evaluation of the difference spectrum shows a decrease in the CD signal at this wavelength for the ribonucleoprotein, which is consistent with a net decrease in base stacking in the P RNA

population due to binding of the C5 protein.^{33,35} Although the difference spectrum shows no significant change in the region of the spectrum associated with protein secondary structure (<230 nm), a complete interpretation is limited by the potential for compensating changes in the CD signal of the RNA subunit.

Loss of RNA base stacking due to complex formation is somewhat surprising given the recent observation that C5 binding stabilizes P RNA folding¹⁸ as structure stabilization would be expected to be associated with an increase in structure content. However, in contrast to results reported for *B. subtilis* P RNA³⁵, CD does not distinguish between formation of secondary and tertiary structure in *E. coli* P RNA (N. Zahler and M. E.H., unpublished results). Nonetheless, the protein-dependent CD change could result from unfolding of RNA that is not linked to holoenzyme formation, or could be due to a net decrease in structure detectable by CD that is associated with an interaction between C5 and a folded, functional form of P RNA. It is, however, possible to exploit the divalent metal ion dependence of tertiary structure formation to shed light on this question.

Previous studies of C5 protein show that Mg^{2+} is not obligatory for its interaction with RNA²⁷; however, concentrations of divalent metal ions greater than 1 mM are required for folding of P RNA into its active conformation and formation of the active holoenzyme.^{35,37–39} These studies reveal that the presence of monovalent ions is sufficient for formation of secondary structure. Thus, we asked whether the protein-dependent changes in RNA structure observed in the CD spectra depend on prior formation of P RNA tertiary structure by comparing the effect of the protein on the observed RNA spectra obtained in the presence and absence of Mg^{2+} .

As shown in Figure 6(b) addition of 17 mM MgCl_2 to the free RNA in buffer alone results in a significant increase in CD signal at 260 nm that is attributed to an increase in base stacking that accompanies RNA folding (curve 4 versus curve 1). Similarly, addition of 100 mM NaCl (curve 2) also results in an increase in the CD signal at 260 nm consistent with increased RNA base stacking. Importantly, the protein-dependent decrease in the CD spectrum of the RNA is only observed in the presence of MgCl_2 , as revealed by comparison of the foregoing results with the spectra for the combined RNA and protein in buffer alone (curve 5), in 100 mM NaCl (curve 3) and in 17 mM MgCl_2 (curve 6). The results clearly show that the protein-dependent decrease in CD at 260 nm is only observed when the RNA is previously folded in Mg^{2+} . Since tertiary folding of the RNA into a functional conformation requires Mg^{2+} , these data suggest that the change in CD signal observed upon addition of protein results from interaction between the C5 protein and a form of the RNA subunit in which some extent of tertiary structure has formed.

Changes in RNA structure indicated by the changes in CD signal upon RNase P protein binding are consistent with previous structure probing and chemical protection experiments showing changes in the chemical protection pattern of the RNA subunit in the presence of the protein.^{12,13,20} The changes in CD signal are likely attributable to the changes in structure that accompany holoenzyme formation. However, it is essential to consider the ability of RNA to form alternate energetically equivalent conformers and to form stable mis-folded states that can be separated from the native conformation by large energetic barriers.^{40,41} Thus, the CD results may reflect a large portion of the population that undergoes relatively small changes in structure upon protein binding. Alternatively, a small portion of the population undergoes a large-scale change in structure while the majority of the population is static. Given the small size of the protein and the high efficiency of formation of the specific functional 1:1 holoenzyme complexes in the presence of divalent metal ion, the latter scenario seems less likely. Thus, the data presented in Figure 6 provide further evidence for protein-dependent changes in P RNA conformation that result from interactions between C5 and the native, folded form of the RNA subunit.

Binding to P RNA stabilizes the folding of C5 protein

Previous physical studies of *B. subtilis* RNase P protein provide evidence that, under conditions where the folded and unfolded protein are in equilibrium, binding of anions is stronger to the folded state and accordingly increasing concentrations of anions shift the equilibrium towards folding.²⁶ An analogous mechanism in which the RNA has a greater affinity for the folded form of the protein is likely to explain the spectroscopic changes associated with *E. coli* RNase P assembly observed here. This model is essentially a classical induced-fit binding mechanism^{1,42} and should necessarily result in increased stability for the bound protein relative to the folded protein free in solution. To test this hypothesis it is necessary to compare the thermal melting of the free protein with that of the protein bound to P RNA.

Typically, thermal melting profiles are obtained from monitoring CD signals related to protein structure as a function of temperature, as done for the free C5 protein in Figure 4(b). A potentially complicating factor for the RNase P holoenzyme is that the large P RNA contributes significantly to the CD signal of the holoenzyme. However, the contribution of RNA to the spectrum is least at 222 nm (Figure 6(a), curve 1) where C5 protein shows an obvious signal (Figure 4(a), curve 2; and Figure 6(a), curve 3); consequently, evaluation of the CD signal at this wavelength should provide information about changes in protein folding. Thus, determination of the temperature dependence of the CD signal

at 222 nm and at 265 nm, a wavelength that is dominated by the RNA signal, permits the thermal melting of the C5 and P RNA subunits of the holoenzyme to be monitored simultaneously.

The thermal melting profile for the holoenzyme monitored at wavelengths specific for the RNA and protein subunits is shown in Figure 7. The data clearly show that the signal at 222 nm, which monitors the protein subunit, reveals a transition that occurs with a T_m of ca 57 °C. The fact that the T_m for the C5 subunit in the holoenzyme is much higher than that observed for the free C5 (34 °C) provides strong support for stabilization of the folded protein by RNA binding as hypothesized. These data also clearly show a transition resulting in a significant decrease in the CD signal at 265 nm, which monitors the RNA subunit, occurs with a very similar T_m (ca 60 °C) to the transition observed at 222 nm. The significant decrease in CD indicates a large decrease in base stacking of the RNA population consistent with thermal unfolding. A decrease in CD at 265 nm is also observed with P RNA alone that occurs with a T_m that is similar (ca 66 °C) to that observed in the presence of C5 protein. Nonetheless, the observation that C5 in the context of the RNase P holoenzyme undergoes a thermal melting transition at essentially the same T_m as that of P RNA provides compelling evidence that unfolding of the two subunits is coupled. The fact that the signal at 265 nm for P RNA decreases with temperature supports coupling of protein and RNA melting. If the protein simply dissociated due to thermal melting without the RNA unfolding, then the P RNA signal at 265 nm should increase based on the data presented in Figure 6(a). Importantly, these data provide strong evidence that the binding of the

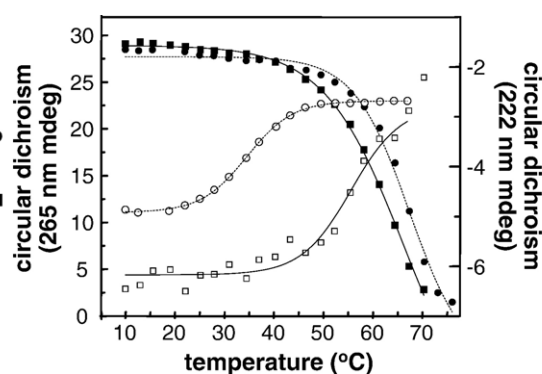


Figure 7. Thermal denaturation spectra of RNase P holoenzyme. CD values of RNase P holoenzyme, P RNA alone and C5 alone (all at 1.5 μ M) in 20 mM sodium cacodylate (pH 6.1), 100 mM NaCl, 1 mM MgCl₂ were monitored at a range of temperatures (10–75 °C). The changes in signal at 222 nm (open symbols) and 265 nm (filled symbols) are shown for the free RNA and protein subunits (circles) and in the context of the RNase P holoenzyme (squares). Thermal melting analyses for both the holoenzyme and free subunits were performed in 1 mM MgCl₂ to suppress metal ion-dependent degradation of P RNA.

RNA subunit stabilized the folding of C5 protein as predicted.

Discussion

The spectroscopic data presented above provide strong evidence that formation of the active *E. coli* holoenzyme involves conformational changes in both the RNA and protein subunit, and that binding of the RNA subunit stabilizes the folding of C5. Recently, Pace and Buck have shown that binding of C5 can alter the folding of P RNA, which is likely to be related to the changes in RNA structure revealed by changes in the CD spectrum, as well as previously observed differences in patterns of chemical protection for the holoenzyme and ribozyme.^{18,20,21} By considering the assembly process as a generalized double two-state, mutual induced-fit model the linkage between RNA binding and stabilization of C5 folding is made more clear. In such a mechanism, the favorable free energy of forming the active complex counterbalances the unfavorable free energies associated with conformational changes in the protein and RNA. In the generalized scheme shown in Figure 8 there are two states for both the RNA and protein components, indicated as 1 and 2. In the case of C5, these states correspond to the denatured protein and to the folded/functional conformation that exists when bound to P RNA, respectively. For P RNA the two states correspond to those that precede and result from the protein-induced conformational change identified in the CD spectrum of the bases at 260 nm. The unimolecular equilibrium constants for the conformational changes between states 1 and 2 are identified as K_P and K_R for the uncomplexed protein and RNA, respectively. The equilibrium dissociation constants for the different complexes are denoted by the subscripted pair of numbers reflecting the conformational state of the RNA and protein, respectively (i.e. $K_{D_{2,1}}$ is the dissociation constant for the active conformation of P RNA and the unfolded conformation of C5). The other equilibrium constants for interconversion of the bound RNA and protein conformations are necessarily determined by those presented. For example, as shown, the equilibrium constant for the conversion of a complex in which the functional form of the RNA is bound by the unfolded protein ($\text{RNA}_2 \cdot \text{Prot}_1$) to the active form of the ribonucleoprotein complex ($\text{RNA}_2 \cdot \text{Prot}_2$) is given by $K_P(K_{D_{2,1}}/K_{D_{2,2}})$.

For C5 the value of K_P is unity at the T_m detected in the melting curve, less than unity above this temperature and greater than unity at lower temperatures. For the P RNA it is presumed that the value of K_R is less than unity, since if it were much greater than unity then it would not be possible to detect a conformational change upon formation of the RNA-protein complex. If it is assumed that the affinity of the folded, active conformations of C5 and P RNA is much greater than when either or both of the components is in its

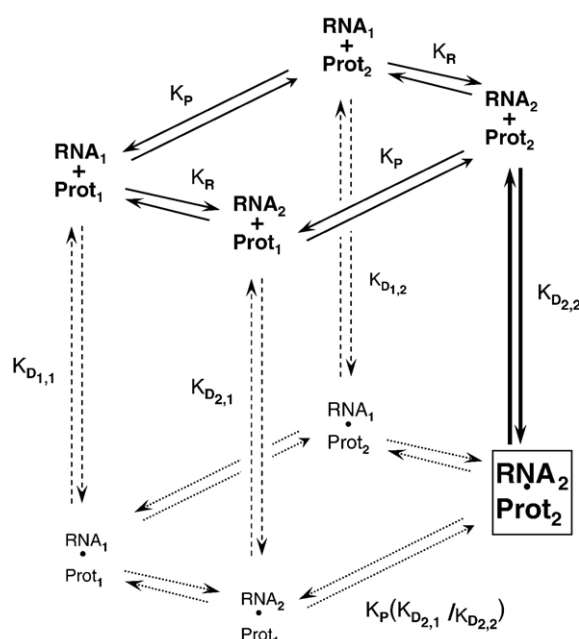


Figure 8. A generalized double two-state, induced-fit model for formation of the RNase P holoenzyme. Two states for both the RNA and protein components are indicated as 1 and 2, respectively. The equilibrium constants for the conformational changes between states 1 and 2 are identified as K_P and K_R for the uncomplexed protein and RNA, respectively. The equilibrium dissociation constants for the different complexes are denoted by the subscripted pair of numbers reflecting the conformational state of the RNA and protein, respectively. Bold lines indicate the favorable interaction between the folded RNA and protein states. Broken lines are used to indicate the unfavorable interactions involving the RNA_1 and Prot_1 states with each other as well as with RNA_2 and Prot_2 , while dotted lines indicate the equilibria between the resulting infrequently populated states. The native, functional holoenzyme complex is boxed.

inactive conformation (i.e. $K_{D_{2,2}} \ll K_{D_{1,1}}, K_{D_{1,2}}$ and $K_{D_{2,1}}$), so that $K_P(K_{D_{2,1}}/K_{D_{2,2}})$ and $K_R(K_{D_{1,2}}/K_{D_{2,2}})$ are both greater than or equal to unity, then only the forms in bold and connected by the filled arrows will be extensively populated at equilibrium. That is, in this simple scheme the conformational changes that result in formation of the active forms occur in the free RNA and protein subunits.

Importantly, the overall equilibrium constant for the limiting free, non-active conformation of either the RNA or protein subunits to form the functional ribonucleoprotein complex ($K_{a,app}$) is given by:

$$\begin{aligned} \frac{[\text{R}_2 \cdot \text{P}_2]}{[\text{R}_1 \text{ or } \text{P}_1]_{\text{lim}}} &= K_{a,app} \\ &= K_P K_R ([\text{R}_2 \text{ or } \text{P}_2]_{\text{ex}} / K_{D_{2,2}}) \quad (1) \end{aligned}$$

where $[\text{R}_2 \text{ or } \text{P}_2]_{\text{ex}}$ indicates the concentration of the free binding partner present in excess and $[\text{R}_1 \text{ or } \text{P}_1]_{\text{lim}}$ is the limiting concentration of the free non-active conformation of the corresponding

RNA or protein. By definition, for the observed induced-fit mechanism to be operative this equilibrium constant must be greater than or equal to unity, while K_P and K_R are less than unity. Converting the equilibrium constants to free energies yields equation (2):

$$K_{a,app} = \exp(-[\Delta G^{\circ}_P + \Delta G^{\circ}_R - \Delta G_{D2,2}]/RT) \quad (2)$$

This relationship clearly shows how the favorable free energy for formation of the active ribonucleo-protein complex offsets the unfavorable free energies associated with the necessary conformational changes in the RNA and protein subunits. Thermodynamically, this would be manifested as an increase in the observed T_m for the protein. During thermal melting disruption of RNA structure that is contacted by the protein is likely to weaken binding affinity. As these RNA-protein interactions are lost the protein will ultimately dissociate and unfold in a transition that is coupled to changes in RNA structure. Thus, this general scheme provides a rationale for the observed increase in thermal stability of C5 in the presence of P RNA and the coupled unfolding of the RNA and protein subunits of the holoenzyme complex. Additionally, it presents a simple context within which to more fully explore the coupling between RNA and protein structural changes.

Because the present analysis of RNase P assembly involved equilibrium measurements, the actual kinetic pathway to forming the active complex, RNA₂-Prot₂, is not specified and cannot yet be identified by the available data. To distinguish whether complexes that are minimally populated at equilibrium (e.g., a complex of folded C5 with the more populated conformation of P-RNA (RNA₁·Prot₂)) contribute to the assembly pathway requires kinetic analysis of the time-course of the association reaction. Importantly, the identified spectroscopic changes that occur during the conformational changes in C5 and P RNA will permit stopped-flow analyses to characterize the pathway of complex assembly.

Such coupled conformational changes during RNA-protein interactions are not unique to RNase P assembly. For example, RNA binding proteins that contain the common RRM motif, as well as their RNA targets, can undergo both large-scale and small-scale dynamics associated with RNA binding. A well studied example is nucleolin, which has two RRMs connected by a linker that is flexible in the free protein but becomes ordered in the nucleolin-RNA complex concomitant with similar disorder/order transitions in the two RRM motifs.^{43,44} Both local and global transitions are driven by interactions with the RNA, which also undergoes conformational changes upon binding.⁴⁵ Molecular dynamics simulations show that correlated motions involving both the RRM and its RNA ligand could account in part for the thermodynamic coupling observed for complex formation.^{46,47} In an additional example, thermal denaturation studies indicate that the free ribosomal protein L5 is not fully structured and

association with 5 S rRNA increases its T_m . As observed for P RNA during RNase P holoenzyme assembly, L5 induces changes in the CD spectrum of 5 S rRNA upon binding. However, coupled conformational changes are not an obligatory mechanism for RNA-protein interactions. For example, the structure of free *M. jannaschii* L7Ae ribosomal protein is essentially identical to that of the RNA-bound protein. However, CD experiments show that the box C/D and C'/D' RNA motifs to which it binds do undergo conformational changes when L7Ae is present.^{36,48} Additionally, analysis of the structures of the common double-stranded RNA binding motif show little change in overall structure between free and bound states.⁴⁹ Similarly, CD and NMR analyses of the complex between double-stranded RNA and the N-terminal domain of the NS1 protein from influenza A virus reveal that NS1 binds without significant conformational changes.⁵⁰ Thus, recognition of the range of dynamics observed underscores the point that achieving a complete understanding of biologically important RNA-protein interactions will require detailed comparative analysis of multiple examples.

This range of dynamic behavior observed in ribonucleoprotein assembly has resulted in terms used in the literature that generally describe the degree of pre-organization present in the free RNA or protein population. Such descriptions range from classical "induced-fit", in which the free conformation is assumed to have only a subset of its structure pre-organized for binding while the rest of the structure is disordered or in an alternative conformation, to "lock and key" describing the other boundary condition, in which the structures of the free and bound states are identical.^{1,2,51,52} Recognition of the potential for conformational heterogeneity of RNA and protein populations gives rise to the idea of "conformational capture", or "kinetic trapping", which describes situations in which the free RNA or protein exists in an ensemble of states in equilibrium, some of which are pre-organized for binding. Binding occurs preferentially to the organized, or folded state, and as molecules equilibrate and assume the correct conformation they are bound and trapped.² Aspects of these descriptions can be recognized in the equilibrium spectroscopic data for RNase P assembly presented here. The free C5 protein is clearly a mixture of folded and unfolded forms in the absence of the RNA subunit, and its binding to P RNA could be described as having characteristics of conformational capture. The folded form is assumed to be pre-organized for binding, although it must be recognized that these data do not indicate whether further conformational changes occur subsequent to binding. With respect to P RNA, the spectroscopic data suggest that the free RNA conformation(s) are stable and distinct from the protein-bound conformation. The observations of good catalytic activity and monophasic kinetics support the assumption that the majority of the RNAs are not significantly mis-folded. Interestingly, the decrease in CD upon protein binding indicates

loss of base stacking consistent with recent chemical probing studies, which support conformational changes in the catalytic core near the binding site for the protein. A plausible model would be that the free RNA adopts a stable conformation competent for catalysis but is unable to form the full set of contacts with the substrate. New interactions with the protein would provide the driving force for breaking interactions necessary for a conformational change permitting new or optimal contacts with the pre-tRNA substrate and stabilizing the folded RNA. Thus, a relatively simple induced-fit mechanism in which the RNA must rearrange to form the full complement of stabilizing RNA-protein interactions is suggested. Although an important first step, equilibrium spectroscopic data alone do not provide a complete description of the assembly pathway, or the mechanisms by which conformational changes are linked to function. An important future direction will be to define the kinetic mechanism of RNase P holoenzyme assembly including the presence and structures of intermediates, as well as to understand the thermodynamic forces driving formation of functional ribonucleoprotein complexes.

Materials and Methods

Purification and characterization of C5 protein

E. coli RNase P protein C5 was purified using the Impact (NEB) expression system. Briefly, the protein was expressed as a fusion with chitin-binding domain and purified by affinity chromatography with subsequent removal of the affinity tag by intein cleavage. The *E. coli* RNase P protein gene (RNPA) was amplified by PCR from the plasmid p930/C5, a generous gift from the Pace laboratory, using the primers RNPANCOF, 5'-TACGCATGCCATGGTTAAGCTCGCATTTCCC-3' and RNPASAPR, 5'-ATCGCTGGGCTCTCCGCAGGACCC-GCGAGCCAGGCGAC-3', which generated restriction sites flanking the gene. The gene was cloned into the Impact (NEB) expression vector pTYB3 as a *SapI*/*NcoI* DNA fragment using standard procedures to generate the plasmid pMHRNPAP.

For expression and subsequent purification, *E. coli* ER2566 (NEB) was transformed with pMHRNPAP. LB broth (12 l) was inoculated and grown at 37 °C to an $A_{600\text{nm}}$ of 0.5–0.8. Expression was then induced by addition of IPTG to 0.3 mM, and incubation was continued at ambient temperature (22–25 °C) for an additional 6 h. The cells were harvested by centrifugation at 5000g for 10 min, and the pellets were frozen at –80 °C.

To assist in lysis, cell pellets were subjected to three freeze-thaw cycles (–80 °C to ambient). For each liter of starting culture pellets were resuspended in 25 ml of Buffer A (20 mM Tris-Cl (pH 8.0), 2 M NaCl, 0.1 mM EDTA, 0.1% reduced Triton X-100 (Calbiochem)) in which 1 COMPLETE protease inhibitor tablet (Roche) was dissolved. Cells were disrupted by sonication on ice, and the sonicate was clarified by centrifugation at 20,000g for 1 h at 4 °C. The lysate was loaded onto a 40 ml bed of Chitin beads (NEB) in a 20 cm × 2.5 cm Kontes Flex column using a Pharmacia FPLC system. The column was first equilibrated with ten column volumes of Buffer A at 1 ml/min. The lysate was loaded at 0.5 ml/min and washed

with 20 column volumes of Buffer A (1 ml/min) followed by two volumes of Buffer B (20 mM Tris-HCl (pH 8), 500 mM NaCl, 0.1 mM EDTA, 0.01% reduced Triton X-100). The column was flushed by gravity flow with three volumes of Buffer B containing 50 mM fresh DTT. Flow was stopped, and the column was incubated in this buffer for 16 h at 4 °C. At this point C5 protein was eluted from the column with five column volumes of Buffer B containing 5 mM fresh DTT (0.5 ml/min). Fractions were collected during this elution, and the peak of C5 protein identified by SDS-PAGE. Peak fractions were pooled and dialyzed in membrane cassettes with a 7000 molecular weight cut-off (Slide-a-lyzer; Pierce) against 1 l of Buffer B containing 5 mM DTT for 2 h at room temperature with one change of dialysis buffer. Dialysis proceeded against 1 l of Buffer B containing 5 mM DTT and 50% glycerol (Storage buffer) for 1 h at room temperature and then overnight at 4 °C with fresh cold buffer. The dialyzed protein in storage buffer was clarified by centrifugation at 20,000g for 2 h at 4 °C. The recovered supernatant was then centrifuged at 20,000g for an additional 3 h. The final supernatant was aliquoted and stored at –20 °C. C5 protein was quantified using the Non-interfering protein assay (Genotech) according to the supplier's instructions. The average yield was ca 2.3 mg of purified protein from 1 l of cell culture with peak fractions ranging from 100–244 μM. The protein remains soluble under these conditions for up to 15 months as indicated by re-quantification after centrifugation.

Kinetic and thermodynamic analyses

RNase P RNA and pre-tRNA^{ASP} substrate used in this study were generated by *in vitro* transcription as described.⁵³ Equilibrium dissociation constants were determined by gel filtration also as described.⁵⁴ Briefly, chromatography using G-100 Sephadex was used to separate the substrate (pre-tRNAs and mature tRNAs) bound to enzyme from free substrate. Experiments were performed in 50 mM Mes (pH 5.75), 100 mM NaCl, 17.5 mM CaCl₂. RNase P RNA, in a series of increasing concentrations, and 5'-³²P-end-labeled pre-tRNA or tRNA at concentrations $<0.2 \times K_{d,\text{app}}$ were renatured separately in the presence of 100 mM NaCl, 50 mM Mes (pH 5.75) (0.005% Triton X-100 for holoenzyme), by heating to 95 °C for 3 min followed by incubation at 37 °C for 10 min. CaCl₂ was added to the desired concentration, and incubation at 37 °C was continued for an additional 10 min. For holoenzyme reactions, C5 protein was added at this point to the same concentrations as RNase P RNA, and the reaction incubated an additional 10 min. Substrate and enzyme were mixed and incubated for 10 min at 37 °C before loading the reactions on spin columns containing 0.7 ml of packed G100 Sephadex equilibrated in 50 mM Mes (pH 5.75), 100 mM NaCl, 17.5 mM CaCl₂. Columns were spun for 25 s at 1200g. Enzyme-substrate complexes in the flow-through and free substrate in the column were subsequently recovered, and the fraction of bound RNA was determined by Cerenkov scintillation counting. The fractions of bound substrate were fit to:

$$F_{\text{bound}} = \text{cpm}_{(\text{flow through})} / (\text{cpm}_{(\text{flow through})} + \text{cpm}_{(\text{column})}) \\ = A + B / (1 + K_d / [E]) \quad (3)$$

where $\text{cpm}_{(\text{flow through})}$ is the amount of radioactive substrate detected in the column flow through and $\text{cpm}_{(\text{column})}$ is the amount of radioactive substrate remaining in the column, A and B are variables which represent

the background of F_{bound} at $[E]=0$ and the maximal fraction bound at $[E]=\text{infinity}$, respectively, K_d is the apparent dissociation constant and $[E]$ is the enzyme concentration.

Single turnover kinetic analyses were performed essentially as described.⁵⁵ Rates were measured in 50 mM Mes (pH 5.75), 100 mM NaCl, 17.5 mM MgCl_2 . Substrate concentrations were 4–6 nM, and enzyme concentrations were greater than fivefold over the $K_{d,\text{app}}$ for the ribozyme and holoenzyme. RNase P RNA and $5'$ - ^{32}P -end-labeled pre-tRNA mixtures were re-natured separately and processed as described above except MgCl_2 was used as the divalent metal ion. Enzyme and substrate were mixed together to start the reaction, and aliquots were removed and quenched with EDTA at a concentration at least twice that of Mg^{2+} . The quenched reaction products were resolved by denaturing gel electrophoresis (15%, w/v), followed by quantification using a Molecular Dynamics phosphorimager system and ImageQuant software, and plotted using KaleidaGraph software. Data were fit to the single exponential function:

$$F_c = A + B e^{-kt} \quad (4)$$

where F_c is the fraction of substrate cleaved, A is background at $t=0$, B is the amplitude of the exponential, k is the observed cleavage rate constant, and t is time. All reported rates and equilibrium binding constants are the average of at least four measurements with less than 30% error in the curve fitting parameters.

Circular dichroism and fluorescence spectroscopy

CD spectra were collected on an Applied Photophysics π^* -180 (UK) or Jasco J-810 spectrometer at 37 °C or 20 °C in 20 mM sodium cacodylate (pH 7.5 or 6.1) in the presence or absence of 100 mM NaCl and 17 mM MgCl_2 or 1 mM MgCl_2 as indicated in the text and Figure legends. The concentrations of C5 protein, P RNA and RNase P holoenzyme (prepared by mixing equimolar C5 and P RNA as described above) were 0.5–1.5 μM as indicated in the Figure legends. Samples were equilibrated at 37 °C for ca 30 min before measurement. Spectra were collected from 200–320 nm for P RNA and 200–260 nm for C5 protein in a 5 mm quartz cuvette at 0.2 nm increments. The sample size was set to 500 with an error of ± 0.0001 and a sample period of 25 μs . The entrance and exit slits were 1 nm. Thermal melts for the C5 protein alone were monitored at 222 nm from 10–60 °C (± 0.1 °C) while those for the RNase P holoenzyme were monitored at both 222 nm and 265 nm from 10–75 °C (± 0.1 °C) at 2–3 °C increments. Thermal melting analyses for both the holoenzyme and free RNA and protein subunits shown in Figure 7 were performed in 1 mM MgCl_2 to suppress metal ion-dependent degradation of P RNA. The integrity of the RNA subunit was monitored by inclusion of a small amount of radiolabeled RNA, which was subsequently analyzed by gel electrophoresis. An equilibration time of 15 min at each temperature was used throughout the melt. The T_m for the CD transitions for the free protein and the holoenzyme was determined by fitting the data to a sigmoidal function:

$$\text{mdeg} = A + (B - A)/(1 + \exp((T - T_m)/dx)) \quad (5)$$

where mdeg is the CD signal at a given temperature, A and B are the minimal and maximal CD signals, respectively, T_m is the temperature at the midpoint of the transition, T is the temperature, and dx is the range of

CD signal over which 75% of the temperature-dependent change occurs.

Fluorescence emission spectra were collected on a Fluoromax-2 spectrometer (Jobin YVON-spex Instruments S.A., Inc.) at 37 °C in a 1 cm quartz cuvette. Concentrations of C5 protein and holoenzyme were 0.5 μM in 20 mM sodium cacodylate (pH 7.5), 100 mM NaCl, 17 mM MgCl_2 . Excitation and emission slit widths were set to 5 nm. The concentration dependence of intrinsic C5 fluorescence was determined at 37 °C with 0.45 μM C5 and 0–1.5 μM P RNA (i.e. ratios of RNA: protein from 0–3). Samples were equilibrated at 37 °C for 30 min prior to analysis.

Acknowledgements

This work was supported by NIH grant GM07645 to M.E.H. We thank Drs Dan Herschlag, Phil Bevilacqua, Mark Caprara, Amy Buck and the members of the Harris laboratory for helpful discussions. We are grateful to Drs Terry Oas, Norman Pace and Amy Buck for sharing results prior to publication. We thank Dr Michael Zagorski for assistance and advice on collection of CD spectra.

References

- Williamson, J. R. (2000). Induced fit in RNA-protein recognition. *Nature Struct. Biol.* **7**, 834–837.
- Leulliot, N. & Varani, G. (2001). Current topics in RNA-protein recognition: control of specificity and biological function through induced fit and conformational capture. *Biochemistry*, **40**, 7947–7956.
- Chen, Y. & Varani, G. (2005). Protein families and RNA recognition. *FEBS J.* **272**, 2088–2097.
- Nissen, P., Hansen, J., Ban, N., Moore, P. B. & Steitz, T. A. (2000). The structural basis of ribosome activity in peptide bond synthesis. *Science*, **289**, 920–930.
- Recht, M. I. & Williamson, J. R. (2004). RNA tertiary structure and cooperative assembly of a large ribonucleoprotein complex. *J. Mol. Biol.* **344**, 395–407.
- Schroeder, R., Barta, A. & Semrad, K. (2004). Strategies for RNA folding and assembly. *Nature Rev. Mol. Cell. Biol.* **5**, 908–919.
- Klein, D. J., Moore, P. B. & Steitz, T. A. (2004). The roles of ribosomal proteins in the structure assembly, and evolution of the large ribosomal subunit. *J. Mol. Biol.* **340**, 141–177.
- Harris, M. E. & Christian, E. L. (2003). Recent insights into the structure and function of the ribonucleoprotein enzyme ribonuclease P. *Curr. Opin. Struct. Biol.* **13**, 325–333.
- Hsieh, J., Andrews, A. J. & Fierke, C. A. (2004). Roles of protein subunits in RNA-protein complexes: lessons from ribonuclease P. *Biopolymers*, **73**, 79–89.
- Gopalan, V., Vioque, A. & Altman, S. (2002). RNase P: variations and uses. *J. Biol. Chem.* **277**, 6759–6762.
- Day-Storms, J. J., Niranjanakumari, S. & Fierke, C. A. (2004). Ionic interactions between PRNA and P protein in *Bacillus subtilis* RNase P characterized using a magnetocapture-based assay. *RNA*, **10**, 1595–1608.

12. Biswas, R., Ledman, D. W., Fox, R. O., Altman, S. & Gopalan, V. (2000). Mapping RNA-protein interactions in ribonuclease P from *Escherichia coli* using disulfide-linked EDTA-Fe. *J. Mol. Biol.* **296**, 19–31.
13. Rox, C., Feltens, R., Pfeiffer, T. & Hartmann, R. K. (2002). Potential contact sites between the protein and RNA subunit in the *Bacillus subtilis* RNase P holoenzyme. *J. Mol. Biol.* **315**, 551–560.
14. Xiao, S., Scott, F., Fierke, C. A. & Engelke, D. R. (2002). Eukaryotic ribonuclease P: a plurality of ribonucleo-protein enzymes. *Annu. Rev. Biochem.* **71**, 165–189.
15. Crary, S. M., Niranjanakumari, S. & Fierke, C. A. (1998). The protein component of *Bacillus subtilis* ribonuclease P increases catalytic efficiency by enhancing interactions with the 5' leader sequence of pre-tRNA^{Asp}. *Biochemistry*, **37**, 9409–9416.
16. Kurz, J. C., Niranjanakumari, S. & Fierke, C. A. (1998). Protein component of *Bacillus subtilis* RNase P specifically enhances the affinity for precursor-tRNA^{Asp}. *Biochemistry*, **37**, 2393–2400.
17. Kurz, J. C. & Fierke, C. A. (2000). Ribonuclease P: a ribonucleoprotein enzyme. *Curr. Opin. Chem. Biol.* **4**, 553–558.
18. Buck, A. H., Dalby, A. B., Poole, A. W., Kazantsev, A. V. & Pace, N. R. (2005). Protein activation of a ribozyme: the role of bacterial RNase P protein. *EMBO J.* **24**, 3360–3368.
19. Kim, J. J., Kilani, A. F., Zhan, X., Altman, S. & Liu, F. (1997). The protein cofactor allows the sequence of an RNase P ribozyme to diversify by maintaining the catalytically active structure of the enzyme. *RNA*, **3**, 613–623.
20. Loria, A., Niranjanakumari, S., Fierke, C. A. & Pan, T. (1998). Recognition of a pre-tRNA substrate by the *Bacillus subtilis* RNase P holoenzyme. *Biochemistry*, **37**, 15466–15473.
21. Tsai, H. Y., Masquida, B., Biswas, R., Westhof, E. & Gopalan, V. (2003). Molecular modeling of the three-dimensional structure of the bacterial RNase P holoenzyme. *J. Mol. Biol.* **325**, 661–675.
22. Kazantsev, A. V., Krivenko, A. A., Harrington, D. J., Carter, R. J., Holbrook, S. R., Adams, P. D. & Pace, N. R. (2003). High-resolution structure of RNase P protein from *Thermotoga maritima*. *Proc. Natl Acad. Sci. USA*, **100**, 7497–7502.
23. Stams, T., Niranjanakumari, S., Fierke, C. A. & Christianson, D. W. (1998). Ribonuclease P protein structure: evolutionary origins in the translational apparatus. *Science*, **280**, 752–755.
24. Spitzfaden, C., Nicholson, N., Jones, J. J., Guth, S., Lehr, R. Prescott, C. D. *et al.* (2000). The structure of ribonuclease P protein from *Staphylococcus aureus* reveals a unique binding site for single-stranded RNA. *J. Mol. Biol.* **295**, 105–115.
25. Gopalan, V., Baxevaris, A. D., Landsman, D. & Altman, S. (1997). Analysis of the functional role of conserved residues in the protein subunit of ribonuclease P from *Escherichia coli*. *J. Mol. Biol.* **267**, 818–829.
26. Henkels, C. H., Kurz, J. C., Fierke, C. A. & Oas, T. G. (2001). Linked folding and anion binding of the *Bacillus subtilis* ribonuclease P protein. *Biochemistry*, **40**, 2777–2789.
27. Talbot, S. J. & Altman, S. (1994). Kinetic and thermodynamic analysis of RNA-protein interactions in the RNase P holoenzyme from *Escherichia coli*. *Biochemistry*, **33**, 1406–1411.
28. Peck-Miller, K. A. & Altman, S. (1991). Kinetics of the processing of the precursor to 4.5 S RNA, a naturally occurring substrate for RNase P from *Escherichia coli*. *J. Mol. Biol.* **221**, 1–5.
29. Jovanovic, M., Sanchez, R., Altman, S. & Gopalan, V. (2002). Elucidation of structure-function relationships in the protein subunit of bacterial RNase P using a genetic complementation approach. *Nucl. Acids Res.* **30**, 5065–5073.
30. Brown, J. W. (1999). The Ribonuclease P Database. *Nucl. Acids Res.* **27**, 314.
31. Gopalan, V., Golbik, R., Schreiber, G., Fersht, A. R. & Altman, S. (1997). Fluorescence properties of a tryptophan residue in an aromatic core of the protein subunit of ribonuclease P from *Escherichia coli*. *J. Mol. Biol.* **267**, 765–769.
32. Lakowicz, J. R. (1999). *Principles of Fluorescence Spectroscopy*. Kluwer, New York.
33. Ratmeyer, L., Vinayak, R., Zhong, Y. Y., Zon, G. & Wilson, W. D. (1994). Sequence specific thermodynamic and structural properties for DNA-RNA duplexes. *Biochemistry*, **33**, 5298–5304.
34. Van Gilst, M., Rees, W. A. & von Hippel, P. H. (1995). Structural and thermodynamic characteristics of the binding of the lambda N protein to a RNA hairpin. *Nucl. Acids Symp. Ser.* **33**, 145–147.
35. Pan, T. & Sosnick, T. R. (1997). Intermediates and kinetic traps in the folding of a large ribozyme revealed by circular dichroism and UV absorbance spectroscopies and catalytic activity. *Nature Struct. Biol.* **4**, 931–938.
36. Suryadi, J., Tran, E. J., Maxwell, E. S. & Brown II, B. A. (2005). The crystal structure of the *Methanocaldococcus jannaschii* multifunctional L7Ae RNA-binding protein reveals an induced-fit interaction with the box C/D RNAs. *Biochemistry*, **44**, 9657–9672.
37. Fang, X., Littrell, K., Yang, X. J., Henderson, S. J., Siefert, S., Thiyagarajan, P. *et al.* (2000). Mg²⁺-dependent compaction and folding of yeast tRNA^{Phe} and the catalytic domain of the *B. subtilis* RNase P RNA determined by small-angle X-ray scattering. *Biochemistry*, **39**, 11107–11113.
38. Fang, X., Pan, T. & Sosnick, T. R. (1999). A thermodynamic framework and cooperativity in the tertiary folding of a Mg²⁺-dependent ribozyme. *Biochemistry*, **38**, 16840–16846.
39. Zarrinkar, P. P., Wang, J. & Williamson, J. R. (1996). Slow folding kinetics of RNase P RNA. *RNA*, **2**, 564–573.
40. Treiber, D. K. & Williamson, J. R. (2001). Beyond kinetic traps in RNA folding. *Curr. Opin. Struct. Biol.* **11**, 309–314.
41. Onoa, B. & Tinoco, I., Jr (2004). RNA folding and unfolding. *Curr. Opin. Struct. Biol.* **14**, 374–379.
42. Fersht, A. (1999). *Structure and Mechanism in Protein Science*. W.H. Freeman and Co., New York.
43. Bouvet, P., Allain, F. H., Finger, L. D., Dieckmann, T. & Feigon, J. (2001). Recognition of pre-formed and flexible elements of an RNA stem-loop by nucleolin. *J. Mol. Biol.* **309**, 763–775.
44. Allain, F. H., Bouvet, P., Dieckmann, T. & Feigon, J. (2000). Molecular basis of sequence-specific recognition of pre-ribosomal RNA by nucleolin. *EMBO J.* **19**, 6870–6881.
45. Finger, L. D., Trantirek, L., Johansson, C. & Feigon, J. (2003). Solution structures of stem-loop RNAs that bind to the two N-terminal RNA-binding domains of nucleolin. *Nucl. Acids Res.* **31**, 6461–6472.
46. Showalter, S. A. & Hall, K. B. (2004). Altering the RNA-binding mode of the U1A RBD1 protein. *J. Mol. Biol.* **335**, 465–480.

47. Showalter, S. A. & Hall, K. B. (2002). A functional role for correlated motion in the N-terminal RNA-binding domain of human U1A protein. *J. Mol. Biol.* **322**, 533–542.
48. Turner, B., Melcher, S. E., Wilson, T. J., Norman, D. G. & Lilley, D. M. (2005). Induced fit of RNA on binding the L7Ae protein to the kink-turn motif. *RNA*, **11**, 1192–1200.
49. Stefl, R., Skrisovska, L. & Allain, F. H. (2005). RNA sequence- and shape-dependent recognition by proteins in the ribonucleoprotein particle. *EMBO Rep.* **6**, 33–38.
50. Chien, C. Y., Xu, Y., Xiao, R., Aramini, J. M., Sahasrabudhe, P. V., Krug, R. M. & Montelione, G. T. (2004). Biophysical characterization of the complex between double-stranded RNA and the N-terminal domain of the NS1 protein from influenza A virus: evidence for a novel RNA-binding mode. *Biochemistry*, **43**, 1950–1962.
51. Weeks, K. M. (1997). Protein-facilitated RNA folding. *Curr. Opin. Struct. Biol.* **7**, 336–342.
52. Herschlag, D. (1988). The role of induced fit and conformational changes of enzymes in specificity and catalysis. *Bioorg. Chem.* **16**, 62–96.
53. Christian, E. L., McPheeters, D. S. & Harris, M. E. (1998). Identification of individual nucleotides in the bacterial ribonuclease P ribozyme adjacent to the pre-tRNA cleavage site by short-range photo-cross-linking. *Biochemistry*, **37**, 17618–17628.
54. Zahler, N. H., Sun, L., Christian, E. L. & Harris, M. E. (2005). The pre-tRNA nucleotide base and 2'-hydroxyl at N(-1) contribute to fidelity in tRNA processing by RNase P. *J. Mol. Biol.* **345**, 969–985.
55. Siew, D., Zahler, N. H., Cassano, A. G., Strobel, S. A. & Harris, M. E. (1999). Identification of adenosine functional groups involved in substrate binding by the ribonuclease P ribozyme. *Biochemistry*, **38**, 1873–1883.

Edited by D. E. Draper

(Received 2 December 2005; received in revised form 25 April 2006; accepted 1 May 2006)

Available online 15 May 2006